JGR Solid Earth

RESEARCH ARTICLE
10.1029/2019JB018267

Effective Pore Fluid Bulk Modulus at Patchy Saturation: An Analytic Study

Leonardo B. Monachesi[1], Uri Wollner[2], and Jack Dvorkin[3]

[1]CONICET, Universidad Nacional de Río Negro. Instituto de Investigación en Paleobiología y Geología, General Roca, Argentina, [2]Department of Geophysics, Stanford University, Stanford, CA, USA, [3]College of Petroleum Engineering and Geosciences, King Fahd University of Petroleum and Minerals (KFUPM), Dhahran, Saudi Arabia

Key Points:
- We derive exact and approximate analytic solutions to model the effective fluid bulk modulus of patchy saturated porous rocks
- We compare and validate the solutions with stochastic simulation and laboratory data

Correspondence to:
J. Dvorkin,
jack.dvorkin@kfupm.edu.sa

Citation:
Monachesi, L. B., Wollner, U., & Dvorkin, J. P. (2020). Effective pore fluid bulk modulus at patchy saturation: An analytic study. *Journal of Geophysical Research: Solid Earth*, *125*, e2019JB018267. https://doi.org/10.1029/2019JB018267

Received 24 JUN 2019
Accepted 21 DEC 2019
Accepted article online 3 JAN 2020

Abstract A patchy saturated two-layered porous rock, with each layer filled with a different fluid, is examined. We assume that this system is probed by an elastic wave having a wavelength much larger than the layers' thicknesses. We also assume that the diffusion length is smaller than the thickness of an individual layer, which implies hydraulic disconnection between layers. In the context of Gassmann's fluid substitution theory, we analytically derived an exact expression for the effective fluid bulk modulus assuming that both layers have the same porosity, dry frame, and mineral matrix properties. In addition we derived an approximate solution that works well at relatively high porosities. Both solutions are expressed as a weighted average of the arithmetic and harmonic averages of individual bulk moduli of the pore fluid. These weights are explicitly given as functions of the porosity, the fractional thicknesses of both layers, and the elastic moduli of the constituents. For the approximate solution, one does not require explicit knowledge of the shear modulus of the rock. The comparison with laboratory data showed that, in the case where a porous, isotropic rock is filled with water and gas, the approximate solution can be used to model the measured data for high values of water saturation.

1. Introduction

Understanding the effects of the pore fluid on the elastic response of fluid-saturated porous rock is crucial to the field of quantitative interpretation of seismic data for reservoir detection and characterization. The theoretical assessment of these effects has been primarily based on the fundamental works by Gassmann (1951) and Biot (1956a, 1956b). These developments have often represented real rock by simple geometries, like concentric cylinders and spheres (e.g., Dutta & Ode, 1979a, 1979b; White, 1975; Vogelaar et al., 2010) and parallel layers (e.g., Gelinsky & Shapiro, 1997; Milani et al., 2016; Norris, 1993; Wollner & Dvorkin, 2016; Wollner & Mavko, 2017). Another type of approximation of real rock is random isotropic porous media composed of two constituents (e.g., Berryman & Milton, 1991).

One important application of Gassmann (1951) work is the ability to predict the elastic response of a fully saturated homogeneous isotropic rock as its single-phase pore fluid is substituted with another and assuming that the rate of rock's deformation is zero. Specifically, Gassmann's equation predicts the elastic response of a rock at different saturating conditions given that its porosity and dry-frame elastic moduli are known and that the pore fluids, as well as the mineral matrix, can be characterized by their bulk moduli. In other words, no matter how many pore fluid or mineral phases are present, they have to have a single bulk modulus for the composite pore fluid and also one for the composite mineral matrix.

Of course, such idealized scenario is rarely found in natural rock, given that it is heterogeneous at all scales. The fluids occupying the pore space can be different in different parts of the rock, and its mineral matrix is usually constituted of multiple minerals. Moreover, the rate of deformation of a porous system is never zero during a dynamic experiment pertinent to elastic wave propagation. Still, the use of Gassmann's fluid substitution appears fairly accurate unless the frequency is very high (ultrasonic) or the viscosity of the fluid is much higher than that of water or conventional oil (e.g., Cadoret, 1993; Lebedev et al., 2009; Müller et al., 2010). Specifically, Gassmann's equations are applicable at instances when the frequency of the wave is sufficiently low such that the characteristic patch size of fluid heterogeneities is much smaller than the diffusion length, thus allowing wave-induced pore-pressure perturbations to equilibrate within a single period of a probing wave (Monachesi et al., 2015; Müller et al., 2010; Rubino et al., 2013).

One approach to relax the single-fluid requirement of Gassmann's theory for a multiphase pore-fluid system is to represent the fluid mixture as a single ideal fluid by assigning to it an effective bulk modulus. An example of such approach is to compute the bulk modulus of a multiphase pore fluid using the Reuss average (Reuss, 1929) of the bulk moduli of individual fluids. Thereafter, this effective bulk modulus $\bar{K}_f$ is used as an input to the Gassmann fluid-substitution equation. This approach inherently assumes that the frequency of the wave that probes the saturated rock allows the wave-induced pore-pressure perturbations to equilibrate within a single period of the probing wave. Numerous studies have validated this approach, including Murphy (1984), Mavko and Mukerji (1998), Müller and Gurevich (2004), and Masson and Pride (2011). It has been found that the Reuss mixing law acts as a lower bound for $\bar{K}_f$.

At instances where the frequency of the probing wave does not allow for sufficient time for the wave-induced pore-pressure perturbations to equilibrate, different fluid-mixture relations were proposed to estimate $\bar{K}_f$ to be used in Gassmann's equation. In all such cases, the wavelength of the probing wave was still assumed to be much larger than local heterogeneities, therefore neglecting any scattering effects on the computed elastic moduli. The idea of applying a different fluid-mixture relation came about as Domenico (1976) experimentally demonstrated that the effective bulk modulus of the brine/gas system deviated from the harmonic averaging scheme of Reuss. This author proposed to use instead the arithmetic averaging of the bulk moduli of the two fluids as an estimate for $\bar{K}_f$. Cadoret (1993) confirmed this finding through laboratory velocity measurements conducted using ultrasonic pulse transmission. Later, Brie et al. (1995) were able to observe this effect in acoustic logging data and proposed another ad hoc fluid-mixing law relating the volume fraction of water in the pore space (S_w) as well as the bulk moduli of gas (K_g) and brine (K_w). Another fluid-mixing relation was recently proposed by Wollner and Dvorkin (2018) based on a numerical study of fluid effects on the elastic response of a porous body. In their numerical experiment, the mineralogy, porosity, and the dry-frame elastic moduli of each layer in a two-layered package were the same. The only difference between the layers was the pore fluid. This study assumed perfect hydraulic isolation between layers, relevant for frequency regimes where the diffusion length of pore fluid filtration in rock is much smaller than the layer thickness. To obtain a fluid-mixing law, Wollner and Dvorkin (2018) first applied Gassmann's equation to each layer to obtain their bulk moduli. Afterward, they applied Hill's (1963) average to the elastic moduli thus computed to obtain the effective bulk modulus of the layered package. In fact, the computed effective bulk modulus of the package is the upper bound for such medium if treated as a homogeneous body. It is also known as the Gassmann-Hill bound explored, for example, by Mavko and Mukerji (1998). Using the effective bulk modulus of the package thus computed, Wollner and Dvorkin (2018) used Gassmann's equation once again to obtain a value for the effective ideal fluid $\bar{K}_f$. Based on their study, the following approximate mixing law was proposed:

$$\bar{K}_f = 0.75K_{f,\mathrm{AR}} + 0.25K_{f,\mathrm{HR}}. \tag{1}$$

In this equation $K_{f,\mathrm{AR}}$ and $K_{f,\mathrm{HR}}$ are the arithmetic (the Voigt upper bound) and harmonic (the Reuss lower bound) averages of the composite pore fluids computed respectively as

$$K_{f,\mathrm{AR}} = f_1K_{f,1} + f_2K_{f,2}, \tag{2}$$

$$K_{f,\mathrm{HR}} = \left(\frac{f_1}{K_{f,1}} + \frac{f_2}{K_{f,2}}\right)^{-1}, \tag{3}$$

where f_1 and $f_2 = 1 - f_1$ are the fractional thicknesses of the layers.

Essentially, the Wollner and Dvorkin (2018) empirical mixing law provided an approximation for the upper bound for the effective bulk modulus of a two-phase fluid that is valid for the layered configuration under examination.

At the same time, it is interesting to find exact values of the coefficients in front of $K_{f,\mathrm{AR}}$ and $K_{f,\mathrm{HR}}$ in the aforementioned mixing law to be used for fluid substitution in the entire layered package. Finding these coefficients under varying properties of the layers will allow to determine an exact expression for the effective bulk modulus for the layered configuration and setting in question, and it is the main problem we pose in this work.

The outline of the paper is as follows: In the next section, we develop an exact representation for $\bar{K}_f$ under similar assumptions as used in Wollner and Dvorkin (2018). For relatively high porosity rocks, we also provide an approximation for $\bar{K}_f$ as a function of the rock's dry *P*wave modulus, porosity, and the volume fraction of the two fluids in the system. Next, in the section 3, we validate the approximate solution via stochastic simulations and compare the results to laboratory data.

Finally, we discuss our results and offer a conclusion.

2. Theory

In this section we start by briefly deriving the effective fluid bulk modulus in the case of a two-layered package in the same way it was recently derived by Wollner and Dvorkin (2018). Once the final expression is obtained, we proceed by deriving an equivalent expression which is a linear combination of $K_{f,\mathrm{AR}}$ and $K_{f,\mathrm{HR}}$.

Let us start by assuming that the porosity ϕ, the bulk modulus of the mineral matrix K_s, and dry-frame bulk and shear moduli K_{dry} and G, respectively, are the same for both layers. If each layer is filled with a different fluid, and the bulk moduli of these fluids are different, then Gassmann's (1951) theory predicts that the saturated rock bulk modulus of layer 1 (K_1) will be different from the corresponding modulus of layer 2 (K_2); meanwhile, the shear modulus will be the same for both layers. As a consequence of the latter condition, the resulting medium is isotropic (Hill, 1963), which implies that the effective compressional modulus of the two-layered system $\bar{M}_{\mathrm{sat}}$ can be computed as the harmonic average of the corresponding individual moduli M_1 and M_2

$$\frac{1}{\bar{M}_{\mathrm{sat}}} = \frac{f_1}{M_1} + \frac{f_2}{M_2}. \tag{4}$$

Given that

$$\bar{M}_{\mathrm{sat}} = \bar{K}_{\mathrm{sat}} + \frac{4}{3}G; \quad \text{and} \quad M_i = K_i + \frac{4}{3}G, \quad i = 1, 2, \tag{5}$$

where $\bar{K}_{\mathrm{sat}}$ represents the effective bulk modulus of the system, equation (4) can be equivalently expressed in terms of bulk moduli as follows

$$\frac{1}{\bar{K}_{\mathrm{sat}} + \frac{4}{3}G} = \frac{f_1}{K_1 + \frac{4}{3}G} + \frac{f_2}{K_2 + \frac{4}{3}G}, \tag{6}$$

from which $\bar{K}_{\mathrm{sat}}$ can be obtained:

$$\bar{K}_{\mathrm{sat}} = \left(\frac{f_1}{K_1 + \frac{4}{3}G} + \frac{f_2}{K_2 + \frac{4}{3}G} \right)^{-1} - \frac{4}{3}G. \tag{7}$$

The bulk moduli of the individual layers, K_1 and K_2, are computed upon K_{dry}, ϕ, and K_s as (Gassmann, 1951)

$$K_i = K_s \frac{\phi K_{\mathrm{dry}} + \left[1 - (1+\phi)K_{\mathrm{dry}}/K_s\right] K_{f,i}}{\phi K_s + \left[(1-\phi) - K_{\mathrm{dry}}/K_s\right] K_{f,i}}, \qquad i = 1, 2. \tag{8}$$

In this equation, $K_{f,i}$ represents the bulk modulus of the fluid contained in the ith layer.

The purpose now is to find the effective fluid bulk modulus $\bar{K}_f$ that, when replaced in Gassmann's fluid substitution equation, will give the effective saturated-rock bulk modulus $\bar{K}_{\mathrm{sat}}$. In order to do so, we assume that the porosity, together with the dry frame and mineral moduli can also be used for the two-layer package considered as a homogeneous body. With these assumptions, we can apply Gassman's equation as follows (e.g., Mavko et al., 2009):

$$\frac{\bar{K}_{\mathrm{sat}}}{K_s - \bar{K}_{\mathrm{sat}}} = \frac{K_{\mathrm{dry}}}{K_s - \bar{K}_{\mathrm{sat}}} + \frac{1}{\phi}\frac{\bar{K}_f}{K_s - \bar{K}_f}, \tag{9}$$

and, as a consequence,

$$\bar{K}_f = K_s \frac{\phi\left(\frac{\bar{K}_{\mathrm{sat}}}{K_s - \bar{K}_{\mathrm{sat}}} - \frac{K_{\mathrm{dry}}}{K_s - K_{\mathrm{dry}}}\right)}{1 + \phi\left(\frac{\bar{K}_{\mathrm{sat}}}{K_s - \bar{K}_{\mathrm{sat}}} - \frac{K_{\mathrm{dry}}}{K_s - K_{\mathrm{dry}}}\right)}, \tag{10}$$

Table 1
Elastic Moduli of the Rock Constituents Employed to Generate the Layered Package

Material	Bulk modulus [GPa]	Shear modulus [GPa]
Quartz	36.6	45
Clay	10.5	3.5
Water	2.61	0
Gas	0.06	0

where $\bar{K}_{\text{sat}}$ is given by equation (7). This last equation gives the effective bulk modulus of the pore fluid for the two-layered package derived by Wollner and Dvorkin (2018). As can be noticed from simple inspection of equations (8), (9), and (10), the dependence of $\bar{K}_f$ upon the pore fluid bulk moduli $K_{f,1}$ and $K_{f,2}$ is rather complicated. However, after algebraic manipulations, it is possible to prove (see the appendix for a detailed derivation) that the following equivalent expression of $\bar{K}_f$ holds

$$\bar{K}_f = \alpha K_{f,\text{AR}} + (1-\alpha) K_{f,\text{HR}}, \tag{11}$$

where the α coefficient appearing in equation (11) is given by

$$\alpha = \frac{\phi M_{\text{dry}}}{\phi M_{\text{dry}} + \left[1 - (1+\phi)\frac{K_{\text{dry}}}{K_s} + \frac{4}{3}\frac{G}{K_s}\left(1 - \phi - \frac{K_{\text{dry}}}{K_s}\right)\right](f_2 K_{f,1} + f_1 K_{f,2})}, \tag{12}$$

and $M_{\text{dry}} = K_{\text{dry}} + \frac{4}{3}G$ is the compressional modulus of the dry frame. Equation (11) is an expression equivalent to equation (10) where the relative contribution of the arithmetic and harmonic averages to the effective bulk modulus of the pore fluid are explicitly given by α. The derivation of this new parameter constitutes the main result of this paper, and as can be seen in equation (12), it is expressed in terms of the porosity, the fractional thicknesses of both layers, and the elastic moduli of the constituents. As a result, equation (12) provides a means to compute the exact relative contributions of $K_{f,AR}$ and $K_{f,HR}$ to the effective fluid bulk modulus of the two-layer package upon the elastic properties of its constituents.

2.1. Approximate Solution

A more convenient expression for α can be obtained if we use the following approximation:

$$\left[1 - (1+\phi)\frac{K_{\text{dry}}}{K_s} + \frac{4}{3}\frac{G}{K_s}\left(1 - \phi - \frac{K_{\text{dry}}}{K_s}\right)\right] \simeq 1. \tag{13}$$

This approximation could be accurate in most cases given that K_{dry}/K_s and G/K_s are typically small compared to 1, although it would be more accurate in the case of high porosity rocks. Using equation (13), α can be approximated by

$$\alpha_{\text{app}} = \frac{\phi M_{\text{dry}}}{\phi M_{\text{dry}} + f_2 K_{f,1} + f_1 K_{f,2}}. \tag{14}$$

Note that equation (14) is very simple and shows that the value for α is mainly controlled by the relative magnitudes of ϕM_{dry} and $f_2 K_{f,1} + f_1 K_{f,2}$. In other words, the approximate solution does not require explicit knowledge of the shear modulus of the rock. This approximation is especially useful if one does not have S wave data to be able to compute the shear modulus of the rock.

In order to evaluate the applicability of equations (13) and (14), in the following section a comparison between the exact and approximate solutions for α is made by considering different rock-physics models. An example of the application of equation (14) is also presented in the next section.

3. Results

3.1. Evaluation of the Applicability of α_{app}

To evaluate the applicability of α_{app}, we perform a comparison between equations (12) and (14) by synthetically generating a two-layered package having the same ϕ, K_s, K_{dry}, and G in both layers. The only difference between layers are their volume fractions f_i and the bulk moduli of the saturating pore fluid $K_{f,i}$ $(i = 1, 2)$.

Table 2
Parameters Employed for Each Rock-Physics Model to Compute the Dry-Frame Elastic Moduli of the Rock Matrix

Model	P_d [MPa]	n	ϕ_c	γ	Ar
Soft Sand	16.5	6	0.4	1	
Stiff Sand	16.5	6	0.4	1	
Constant Cement	16.5	14	0.4	1	
DEM					0.1

Note. P_d is the differential pressure; n is the coordination number; ϕ_c is the critical porosity; γ is the shear correction factor; and Ar is the aspect ratio.

To generate the two-layered package, both the porosity ϕ and the fractional thickness f_1 were randomly varied within the intervals $(0.15, 0.35)$ and $(0, 1)$, respectively. The solid frame was assumed to be composed of a quartz/clay mixture, and the effective bulk modulus K_s was computed as the Hill's average (e.g., Mavko et al., 2009) of the bulk moduli of both constituents. These moduli were computed using the mineral moduli listed in Table 1 and randomly varying the clay content between zero and 100%. Layer 1 was fully saturated with water, meaning that f_1 is equivalent to the water saturation S_w of the package, while Layer 2 was fully saturated with gas. The values for water and gas bulk moduli are also listed in Table 1.

To compute the dry-frame elastic moduli of the system, we employed four different rock-physics models that depend on porosity and mineralogy: Soft Sand (the modified lower Hashin-Shtrikman bound); Stiff Sand (the modified upper Hashin-Shtrikman bound); Constant-Cement (the Soft Sand model with high coordination number); and the Differential Effective Medium (DEM; Mavko et al., 2009). For the computation of these rock-physics models, we employed the model parameters listed in Table 2.

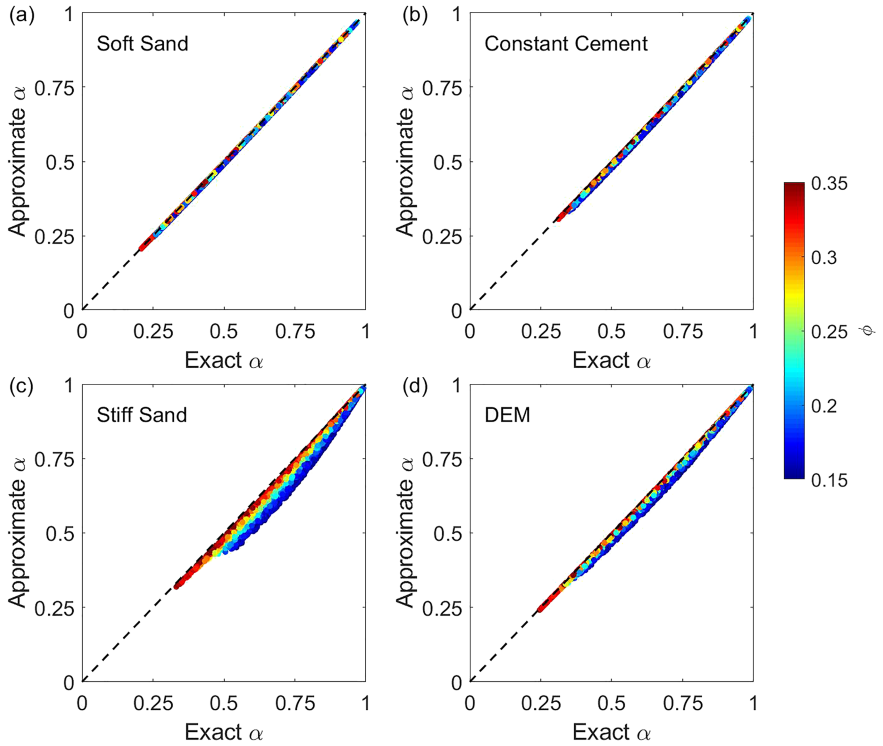

Figure 1. Approximate parameter α_{app} (equation (14)) against the exact α (equation (12)) obtained for multiple statistical realizations of a two-layered package. The elastic properties of each package are generated using a rock-physics model, namely, (a) Soft Sand, (b) Constant Cement, (c) Stiff Sand, and (d) DEM. The difference between any two layers in each package is the saturating fluid. One layer is fully water saturated, whereas the second layer is fully gas saturated. The plotted values are color-coded by porosity values.

Table 3
Poroelastic Parameters of Sample S7 From Cadoret (1993) and Pore Fluids Used in This Study

Variables	Meaning	Value
M_s	Compressional modulus of solid grain	120 GPa
ϕ	Porosity	0.3
κ	Permeability	2.6×10^{-13} m^2
K_w	Bulk modulus of water	2.25 GPa
K_g	Bulk modulus of gas	0.03 GPa
ρ_s	Density of solid	2.7 g/cm^3
ρ_w	Density of water	1 g/cm^3
ρ_g	Density of gas	0.006 g/cm^3

Figure 1 shows a plot of the computed approximate parameter α_{app} obtained from equation (14), against the exact α value obtained from equation (12) for several statistical realizations. These results are color-coded using the porosity values of the package. We observe that regardless of the rock-physics model used, at relatively high porosities (>0.25), equation (14) approximates well the exact solution. This observation is understandable as higher porosity lead to softer rock, thus corroborating the approximation of equation (14).

3.2. Comparison With Experimental Data

Cadoret (1993) exemplified the effect of patchy saturation on the effective elastic properties of rocks obtained from bench top measurements on various carbonate rocks. Cadoret saturated dry rock samples with water, and, at different water saturation levels, he recorded the time it took for a *P* wave to traverse the rock sample from one end of the rock to the other. By measuring the thickness of the sample, Cadoret then computed the velocity of the *P* wave. Patches of water were shown to form as fully water saturated rocks were dried. In this section, we wish to validate the approximate solution α_{app} for one of Cadoret's rock samples that exhibited patchy saturation.

Recall that the underlying requirement of this work is that the examined rock specimen is treated as a homogeneous body having effective elastic and petrophysical properties. In other words, the wavelength of a probing wave is much larger than local heterogeneity within the rock. In addition, we assumed that the fluid saturating regions can be considered to be hydraulically isolated from each other given that the thickness of each region exceeds the diffusion length. That is to say, the interplay between porosity, permeability, dynamic viscosity, and fluid bulk modulus for a given frequency of the probing wave determine whether local fluid patches are hydraulically communicating or not.

Though we had posed our problem as one dealing with layered media, our mathemaical derivations are not limited to this setting as long as our assumptions of the rock properties are met. In our initial problem statement, we required that our two-layered media had both layers with the same ϕ, K_s, K_{dry}, and G. The difference between the layers is the saturating fluid. In other words, we had initially considered the case of layered fluids patches. However, equivalent effective elastic behavior of such rock will be observed if the fluid patches were in a different configuration inside it that are spatially variable. This is the case observed by Cadoret.

Specifically, we chose to examine the bench top measurements performed at 50 kHz by Cadoret for sample Estaillades S7 (Limestone) during drainage process. The rock sample was approximately isotropic. The poroelastic parameters of this sample, as recorded by Cadoret (ϕ, ρ_s, and permeability κ), and other parameters used in this study are given in Table 3. K_w, K_g, ρ_w, ρ_g, and M_s were selected based on studies listed in Mavko et al. (2009).

During his measurements, Cadoret also CT scanned the rock at different water saturation stages. Toms-Stewart et al. (2009) used these images to estimate the spatial correlation length of water patches for Cadoret's partially saturated sample. They noted that it increased with increasing S_w. Later, Kobayashi and Mavko (2016) suggested a power law relation relating the characteristic diffusion length L_c and S_w to fit their model to Cadoret's data. They defined L_c as $L_c = a_0 \times S_w/(1 - S_w)$. This relation shows an increase in L_c with an increase in S_w for given dry rock heterogeneity scale a_0. The term L_c essentially characterizes the

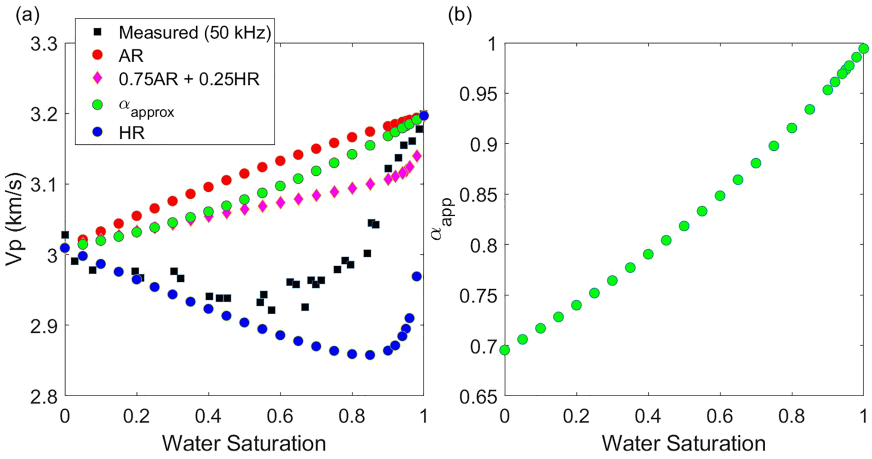

Figure 2. (a) P wave velocity values plotted against the fraction of water saturated pore space. The black markers are those measured by Cadoret (1993) for sample S7 using a 50-kHz transducer showing effect of patchy saturation on measured V_p. The red, green, and blue markers are approximated solutions to the observed V_p-S_w behavior as $\bar{K}_f$ is approximated and then used as input to the V_p-only fluid substitution. $\bar{K}_f$ is approximated as either $K_{f,\mathrm{AR}}$ (red markers), $K_{f,\mathrm{HR}}$ (blue markers), and using equations (14) and (11) (green markers). The magenta markers were computed assuming $\alpha = 0.75$ (equation (1)). (b) The computed α_{app} parameter as a function of water saturation.

patch size of fluid heterogeneities. The larger the characteristic patch size compared to the diffusion length in a rock, the less fluid flow occurs within the rock. Hence, wave-induced pore-pressure perturbations cannot reach equilibrium. In other words, at high water saturation levels we expect to see patchy saturation behavior.

Since Cadoret only measured the P wave velocity of this sample at different saturation levels, we cannot determine the dry bulk modulus of the sample and Gassmann's fluid substitution relations. To overcome this issue, we utilized the approximate Gassmann's fluid substitution equation for isotropic bodies suggested by Mavko et al. (1995), also known as the V_p-only fluid substitution relations, to approximate the dry P wave modulus from the fully gas-saturated rock. This approximation is given by

$$M_{\mathrm{dry}} = \frac{M_{\mathrm{sat}}(\phi M_s/K_g + 1 - \phi) - M_s}{\phi M_s/K_g + M_{\mathrm{sat}}/M_s - 1 - \phi}, \tag{15}$$

where M_s is the P wave modulus of the mineral component comprising the rock and M_{sat} is given by

$$M_{\mathrm{sat}} = V_p^2 \rho_b, \tag{16}$$

with

$$\rho_b = (1-\phi)\rho_s + \phi\rho_g. \tag{17}$$

We then computed α_{app} using equation (14) and the resulting effective fluid bulk modulus of the sample using equation (11). The effective fluid bulk modulus is then used as input to the V_p-only fluid substitution to obtain the P wave modulus of the rock sample at different water saturation stages assuming the gas and water patches are hydraulically disconnected from each other. The resulting P wave velocity is computed as

$$V_p = \sqrt{M_{\mathrm{sat}}/\rho_b}, \tag{18}$$

where

$$M_{\mathrm{sat}} = M_s \frac{\phi M_{\mathrm{dry}} - (1+\phi)\bar{K}_f M_{\mathrm{dry}}/M_s + \bar{K}_f}{(1-\phi)\bar{K}_f + \phi M_s - \bar{K}_f M_{\mathrm{dry}}/M_s}, \tag{19}$$

and ρ_b given by

$$\rho_b = (1-\phi)\rho_s + \phi\left[S_w\rho_w + (1-S_w)\rho_g\right]. \tag{20}$$

These results are shown in Figure 2a along with the measurements recorded by Cadoret (1993). For comparison, we also added the resulting P wave velocity of equations (18) to (20), given the effective fluid bulk modulus of the rock sample is computed either as $K_{f,\mathrm{AR}}$ or $K_{f,\mathrm{HR}}$. Furthermore, we added the resulting P wave velocity relation using equation (1) as suggested by Wollner and Dvorkin (2018).

We observe that patchy saturation with complete hydraulic disconnection between fluid patches can be better estimated using α_{app} (green markers) at high saturations ($S_w > 85\%$), whereas at low saturations, this analytical solution overestimate the measured data. One reason for this observation is that at low values of S_w, the size of the water patches are smaller or comparable to the diffusion length. On the other hand, at high saturation values, the size of the water patches become larger than the diffusion length, resulting in complete hydraulic disconnection; this is the setting we assumed in this study. For further details on the effects of the size of water patches and diffusion length on the measured P wave velocity on a rock, the reader is referred to Müller et al. (2010).

As the α parameter (both in its exact or approximated version) depends on water saturation S_w, there is not a unique value of α in the computation of the the effective fluid bulk modulus of Figure 2a. Figure 2b illustrates this dependence.

We note that the curve generated by equation (1) (Wollner & Dvorkin, 2018) does provide a better match to the V_p data, in this case, than using α_{app} in equation (11). However, we must reiterate that the notion of using α_{app} was to model a complete hydraulic disconnection between water patches. Thus, a deviation from this assumption will likely cause a discrepancy between modeled V_p-S_w dependency and the measured one.

4. Discussion

The main purpose of the present study was to analytically address the effect of the pore fluid distribution on the elastic properties of fluid-saturated porous rock. We focused on the case of a two-layered package where the mineralogy, porosity, and dry-frame elastic moduli were constant and the only difference between the layers was in the pore fluid. We also considered that no hydraulic communication occurs between the layers since it is often associated with the concept of patchy saturation. An important result addressed by Wollner and Dvorkin (2016) was to find an analytic solution that could be used in anisotropic Gassmann's fluid substitution applied to a sequence of layers considered as an anisotropic homogeneous body (equation (10)). Wollner and Dvorkin (2018) provided an exact relation for the effective fluid bulk modulus for a layered package, as is assumed in this study. They also hypothesized that this effective modulus can also be computed as a linear combination of the arithmetic and harmonic averages of the fluid bulk moduli in the individual layers. However, Wollner and Dvorkin (2018) only provided an empirical solution for the weights to be used in the linear fit (equation (1)). The main result of the present study was to analytically develop the weighting coefficients for Wollner and Dvorkin (2018) proposed linear fit and obtain an exact alternative expression for the effective fluid bulk modulus of a two-layered package. These weights are related to each other by the α parameter (equation (12)). This new parameter is explicitly expressed as a function of the porosity, the fractional thicknesses of both layers and the elastic properties of the constituents.

The analytic solution derived for the α parameter was approximated by a rather simpler mathematical expression (equation (14)). It is informative to note that this expression does not require knowledge of the shear modulus of the rock, which makes it specifically useful if one does not have S wave data to be able to compute this modulus.We performed a comparative stochastic analysis between both the exact and the approximate solutions for α by considering four different rock-physics models, The analysis clearly showed that for relatively high porosities α_{app} turns out to be a very good approximation of α, regardless of the model considered. The obtained results are consistent with the approximation made in equation (13), which is more accurate for softer rocks.

The derived analytic solution for $\bar{K}_f$ was tested with experimental data of P wave velocity collected by Cadoret (1993) from a rock sample exhibiting patchy saturation. In order to compare our model predictions with the laboratory data, we computed the V_p velocity as a function of water saturation using the effective fluid bulk modulus predicted by equation (11) with α given by its approximate expression (14). We concluded that when the patches are hydraulically disconnected, the effective fluid bulk modulus can be modeled using α_{app} at high saturations; meanwhile, at intermediate and low saturations, the proposed solution overestimates the experimental data. This result was expected, given that for high saturations, water

patches become larger than the diffusion length, resulting in complete hydraulic disconnection, which is the setting we assume in this study.

5. Conclusion

We derived a new analytic solution for the effective fluid bulk modulus $\bar{K}_f$ to be used in fluid substitution. The solution is valid for a patchy saturated two-layer system where both layers, each filled with a different fluid, are assumed to be hydraulically disconnected. The solution is expressed as a weighted average of the arithmetic and harmonic averages of individual bulk moduli of the pore fluid. We also derived an approximate solution that is very simple and works well at relatively high porosities. This solution does not require knowledge of the shear modulus of the rock, which makes it specifically useful if one does not have S wave data to be able to compute this modulus. We performed a comparison of the approximate solution with laboratory data and showed that for high values of water saturation the solution can be safely used to model the measured data.

As a concluding remark, it is important to mention that the new derived analytic solutions provide a means to estimate the relative contributions of $K_{f,\mathrm{AR}}$ and $K_{f,\mathrm{HR}}$ to the effective fluid bulk modulus of the two-layer package upon the elastic properties of its constituents.

Appendix A: Derivation of Equations (11) and (12)

This appendix includes a full derivation of the equations (11) and (12). We start by defining the following constants:

$$\begin{aligned} A &= \phi K_{\mathrm{dry}}, \quad B = 1-(1+\phi)K_{\mathrm{dry}}/K_s, \\ C &= \phi K_s, \quad D = 1-\phi-K_{\mathrm{dry}}/K_s. \end{aligned} \tag{A1}$$

With them, equation (8) for K_i can be written as

$$K_i = K_s \frac{A+BK_{f,i}}{C+DK_{f,i}}. \tag{A2}$$

Using equation (A2), we can write

$$K_i + \frac{4}{3}G = K_s \frac{\left(A+\frac{4}{3}\frac{G}{K_s}C\right)+\left(B+\frac{4}{3}\frac{G}{K_s}D\right)K_{f,i}}{C+DK_{f,i}}. \tag{A3}$$

Now, let us call for simplicity

$$E = A+\frac{4}{3}\frac{G}{K_s}C, \quad F = B+\frac{4}{3}\frac{G}{K_s}D, \tag{A4}$$

then

$$K_i + \frac{4}{3}G = K_s \frac{E+FK_{f,i}}{C+DK_{f,i}}. \tag{A5}$$

Using this last expression, we can write

$$\begin{aligned} &\frac{f_1}{K_1+\frac{4}{3}G}+\frac{f_2}{K_2+\frac{4}{3}G} \\ &= \frac{1}{K_s}\frac{f_1(C+DK_{f,1})(E+FK_{f,2})+f_2(C+DK_{f,2})(E+FK_{f,1})}{(E+FK_{f,1})(E+FK_{f,2})}, \end{aligned} \tag{A6}$$

from which the inverse results

$$\begin{aligned} &\left(\frac{f_1}{K_1+\frac{4}{3}G}+\frac{f_2}{K_2+\frac{4}{3}G}\right)^{-1} \\ &= K_s \frac{(E+FK_{f,1})(E+FK_{f,2})}{f_1(C+DK_{f,1})(E+FK_{f,2})+f_2(C+DK_{f,2})(E+FK_{f,1})}. \end{aligned} \tag{A7}$$

Now, defining the constants H, I, J, and K as

$$H = E - \frac{8}{3}\frac{G}{K_s}Cf_1, \quad I = F - \frac{8}{3}\frac{G}{K_s}Df_1,$$
$$J = E - \frac{8}{3}\frac{G}{K_s}Cf_2, \quad K = F - \frac{8}{3}\frac{G}{K_s}Df_2, \tag{A8}$$

we obtain for $\bar{K}_{\text{sat}}$ (see equations (7) and (A7))

$$\bar{K}_{\text{sat}} = \frac{K_s}{2}\frac{\left(H + IK_{f,1}\right)\left(E + FK_{f,2}\right) + \left(J + KK_{f,2}\right)\left(E + FK_{f,1}\right)}{f_1(C + DK_{f,1})(E + FK_{f,2}) + f_2(C + DK_{f,2})(E + FK_{f,1})}. \tag{A9}$$

Now, we proceed as follows:

$$\begin{aligned} &K_s - \bar{K}_{\text{sat}} \\ &= \frac{K_s}{2}\left(\frac{\left(E + FK_{f,2}\right)\left[\left(2f_1C - H\right) + \left(2f_1D - I\right)K_{f,1}\right]}{f_1(C + DK_{f,1})(E + FK_{f,2}) + f_2(C + DK_{f,2})(E + FK_{f,1})}\right) \\ &\quad + \frac{K_s}{2}\left(\frac{\left(E + FK_{f,1}\right)\left(\left[2f_2C - J\right] + \left[2f_2D - K\right]K_{f,2}\right)}{f_1(C + DK_{f,1})(E + FK_{f,2}) + f_2(C + DK_{f,2})(E + FK_{f,1})}\right). \end{aligned} \tag{A10}$$

Calling

$$L = 2f_1C - H, \quad M = 2f_1D - I, \quad N = 2f_2C - J, \quad P = 2f_2D - K, \tag{A11}$$

then

$$K_s - \bar{K}_{\text{sat}} = \frac{K_s}{2}\frac{\left(E + FK_{f,2}\right)\left(L + MK_{f,1}\right) + \left(E + FK_{f,1}\right)\left(N + PK_{f,2}\right)}{f_1(C + DK_{f,1})(E + FK_{f,2}) + f_2(C + DK_{f,2})(E + FK_{f,1})}. \tag{A12}$$

Combining equations (A9) and (A12), we obtain

$$\frac{\bar{K}_{\text{sat}}}{K_s - \bar{K}_{\text{sat}}} = \frac{\left(E + FK_{f,2}\right)\left(H + IK_{f,1}\right) + \left(E + FK_{f,1}\right)\left(J + KK_{f,2}\right)}{\left(E + FK_{f,2}\right)\left(L + MK_{f,1}\right) + \left(E + FK_{f,1}\right)\left(N + PK_{f,2}\right)}. \tag{A13}$$

With this last expression we can write

$$\begin{aligned} &\frac{\bar{K}_{\text{sat}}}{K_s - \bar{K}_{\text{sat}}} - \frac{K_{\text{dry}}}{K_s - K_{\text{dry}}} \\ &= \frac{\left(E + FK_{f,2}\right)\left(H + IK_{f,1}\right) + \left(E + FK_{f,1}\right)\left(J + KK_{f,2}\right)}{\left(E + FK_{f,2}\right)\left(L + MK_{f,1}\right) + \left(E + FK_{f,1}\right)\left(N + PK_{f,2}\right)} - \frac{K_{\text{dry}}}{K_s - K_{\text{dry}}} \\ &= \frac{\left(E + FK_{f,2}\right)\left[\left(H - \frac{K_{dry}}{K_s - K_{dry}}L\right) + \left(I - \frac{K_{dry}}{K_s - K_{dry}}M\right)K_{f,1}\right]}{\left(E + FK_{f,2}\right)\left(L + MK_{f,1}\right) + \left(E + FK_{f,1}\right)\left(N + PK_{f,2}\right)} \\ &\quad + \frac{\left(E + FK_{f,1}\right)\left[\left(J - \frac{K_{dry}}{K_s - K_{dry}}N\right) + \left(K - \frac{K_{dry}}{K_s - K_{dry}}P\right)K_{f,2}\right]}{\left(E + FK_{f,2}\right)\left(L + MK_{f,1}\right) + \left(E + FK_{f,1}\right)\left(N + PK_{f,2}\right)}. \end{aligned} \tag{A14}$$

Calling

$$Q = H - \frac{K_{\text{dry}}}{K_s - K_{\text{dry}}}L, \quad R = I - \frac{K_{\text{dry}}}{K_s - K_{\text{dry}}}M,$$
$$S = J - \frac{K_{\text{dry}}}{K_s - K_{\text{dry}}}N, \quad T = K - \frac{K_{\text{dry}}}{K_s - K_{\text{dry}}}P, \tag{A15}$$

we obtain

$$\frac{\bar{K}_{\text{sat}}}{K_s - \bar{K}_{\text{sat}}} - \frac{K_{\text{dry}}}{K_s - K_{\text{dry}}} = \frac{\left(E + FK_{f,2}\right)\left(Q + RK_{f,1}\right) + \left(E + FK_{f,1}\right)\left(S + TK_{f,2}\right)}{\left(E + FK_{f,2}\right)\left(L + MK_{f,1}\right) + \left(E + FK_{f,1}\right)\left(N + PK_{f,2}\right)}. \tag{A16}$$

Then,

$$\begin{aligned}
&1+\phi\left(\frac{\bar{K}_{\text{sat}}}{K_s-\bar{K}_{\text{sat}}}-\frac{K_{\text{dry}}}{K_s-K_{\text{dry}}}\right)\\
&=1+\phi\frac{\left(E+FK_{f,2}\right)\left(Q+RK_{f,1}\right)+\left(E+FK_{f,1}\right)\left(S+TK_{f,2}\right)}{\left(E+FK_{f,2}\right)\left(L+MK_{f,1}\right)+\left(E+FK_{f,1}\right)\left(N+PK_{f,2}\right)}\\
&=\frac{\left(E+FK_{f,2}\right)\left[(L+\phi Q)+(M+\phi R)K_{f,1}\right]+\left(E+FK_{f,1}\right)\left[(N+\phi S)+(P+\phi T)K_{f,2}\right]}{\left(E+FK_{f,2}\right)\left(L+MK_{f,1}\right)+\left(E+FK_{f,1}\right)\left(N+PK_{f,2}\right)},
\end{aligned}\tag{A17}$$

and if we call

$$U=L+\phi Q,\quad V=M+\phi R,\quad W=N+\phi S,\quad X=P+\phi T,\tag{A18}$$

we can express the last equation as follows:

$$\begin{aligned}
&1+\phi\left(\frac{\bar{K}_{\text{sat}}}{K_s-\bar{K}_{\text{sat}}}-\frac{K_{\text{dry}}}{K_s-K_{\text{dry}}}\right)\\
&=\frac{\left(E+FK_{f,2}\right)\left(U+VK_{f,1}\right)+\left(E+FK_{f,1}\right)\left(W+XK_{f,2}\right)}{\left(E+FK_{f,2}\right)\left(L+MK_{f,1}\right)+\left(E+FK_{f,1}\right)\left(N+PK_{f,2}\right)}.
\end{aligned}\tag{A19}$$

Finally, using equations (A16) and (A19) in the expression for $\bar{K}_f$ given by equation (10), we get

$$\bar{K}_f=\phi K_s\frac{(E+FK_{f,2})(Q+RK_{f,1})+(E+FK_{f,1})(S+TK_{f,2})}{(E+FK_{f,2})(U+VK_{f,1})+(E+FK_{f,1})(W+XK_{f,2})}.\tag{A20}$$

This last expression can be simplified given that the constants Q, S, V, and X verify

$$Q+S=0,\quad V+X=0.\tag{A21}$$

Then, $\bar{K}_f$ can be written as

$$\bar{K}_f=\phi K_s\frac{\left(\frac{ER+FS}{f_1}\right)K_{f,1}f_1+\left(\frac{ET+FQ}{f_2}\right)K_{f,2}f_2+F(R+T)K_{f,1}K_{f,2}}{E(U+W)+(EV+FW)f_1\frac{K_{f,1}}{f_1}+(FU+EX)f_2\frac{K_{f,2}}{f_2}}.\tag{A22}$$

Now, calling

$$\begin{aligned}
&Y_1=\frac{ER+FS}{f_1},\quad Y_2=\frac{ET+FQ}{f_2},\\
&Z_1=(EV+FW)f_1,\quad Z_2=(FU+EX)f_2,
\end{aligned}\tag{A23}$$

it is possible to prove that $Y_1=Y_2$ and $Z_1=Z_2$. Let us call them for simplicity Y and Z, respectively. Also, we can prove that the following relations hold

$$E(U+W)=\phi K_sY,\quad \frac{Z}{f_1f_2}=\phi K_sF(R+T).\tag{A24}$$

Then, $\bar{K}_f$ can be written as

$$\bar{K}_f=\frac{\phi K_sY\left(f_1K_{f,1}+f_2K_{f,2}\right)+\frac{Z}{f_1f_2}K_{f,1}K_{f,2}}{\phi K_sY+Z\left(\frac{K_{f,1}}{f_1}+\frac{K_{f,2}}{f_2}\right)}.\tag{A25}$$

Equation (A25) can be rearranged as

$$\bar{K}_f=\frac{\phi K_sY}{\phi K_sY+\frac{Z}{f_1f_2}\left(f_2K_{f,1}+f_1K_{f,2}\right)}K_{f,\text{AR}}+\frac{\frac{Z}{f_1f_2}\left(f_2K_{f,1}+f_1K_{f,2}\right)}{\phi K_sY+\frac{Z}{f_1f_2}\left(f_2K_{f,1}+f_1K_{f,2}\right)}K_{f,\text{HR}},\tag{A26}$$

where $K_{f,\mathrm{AR}}$ and $K_{f,\mathrm{HR}}$ are given by equations (2) and (3), respectively. Using the relations given for the constants defined in (A1), (A4), (A8), (A11), (A15), and (A18), we find

$$\begin{aligned} \phi K_s Y &= 2\phi^2 \left(K_s - K_{\mathrm{dry}}\right)\left(K_{\mathrm{dry}} + \frac{4}{3}G\right), \\ \frac{Z}{f_1 f_2} &= 2\phi \left(K_s - K_{\mathrm{dry}}\right)\left[1 - (1+\phi)\frac{K_{\mathrm{dry}}}{K_s} + \frac{4}{3}\frac{G}{K_s}\left(1 - \phi - \frac{K_{\mathrm{dry}}}{K_s}\right)\right]. \end{aligned} \tag{A27}$$

Replacing the last expressions of (A27) in equation (A26), we obtain the final equations (11) and (12).

Acknowledgments
We thank professor Yves Guéguen and an anonymous reviewer for their constructive comments. J. D.'s work was supported by the Center for Integrative Petroleum Research at King Fahd University of Petroleum and Minerals. The data used in this work are uploaded in the repository (https://data.mendeley.com/datasets/y34czv2f7c/4, DOI: 10.17632/y34czv2f7c.4).

References

Berryman, J. G., & Milton, G. W. (1991). Exact results for generalized Gassmann's equation in composite porous media with two constituents. *Geophysics*, *56*, 1950–1960.

Biot, M. A. (1956a). Theory of propagation of elastic waves in a fluid saturated porous solid, I. Low-frequency range. *Journal of the Acoustical Society of America*, *28*, 168–178. https://doi.org/10.1121/1.1908239

Biot, M. A. (1956b). Theory of propagation of elastic waves in a fluid saturated porous solid, II. Higher-frequency range. *Journal of the Acoustical Society of America*, *28*, 179–191. https://doi.org/10.1121/1.1908241

Brie, A., Pampuri, F., Marsala, A. F., & Meazza, O. (1995). Shear sonic interpretation in gas-bearing sands, *SPE Annual Technical Conference and Exhibition* (pp. 701–710). Dallas, Texas: Society of Petroleum Engineers.

Cadoret, T. (1993). Effet de la saturation eau/gaz sur les propriétés acoustiques des roches (Ph.D. Thesis), University of Paris.

Domenico, S. N. (1976). Effect of brine-gas mixture on velocity in an unconsolidated gas reservoir. *Geophysics*, *41*, 882–894.

Dutta, N. C., & Ode, H. (1979a). Attenuation and dispersion of compressional waves in fluid-filled porous rocks with partial gas saturation (White model) - part I: Biot theory. *Geophysics*, *44*, 1777–1788.

Dutta, N. C., & Ode, H. (1979b). Attenuation and dispersion of compressional waves in fluid-filled porous rocks with partial gas saturation (White model)—Part II: Results. *Geophysics*, *44*, 1789–1805.

Gassmann, F. (1951). Uber die elastizitat poroser medien. *Vierteljahrsschrift der Naturforschenden Gesellschaft in Zurich*, *96*, 1–23.

Gelinsky, S., & Shapiro, S. A. (1997). Poroelastic backus averaging for anisotropic layered fluid- and gas-saturated sediments. *Geophysics*, *62*, 1867–1878.

Hill, R. (1963). Elastic properties of reinforced solids: Some theoretical principles. *Journal of Mechanics and Physics of Solids*, *11*, 357–372.

Kobayashi, Y., & Mavko, G. (2016). Variation in P-wave modulus with frequency and water saturation: Extension of dynamic-equivalent-medium approach. *Geophysics*, *81*, D479–D494. https://doi.org/10.1190/GEO2015-0045.1

Lebedev, M., Toms-Stewart, J., Clennell, B., Pervukhina, M., Shulakova, V., Paterson, L., et al. (2009). Direct laboratory observation of patchy saturation and its effects on ultrasonic velocities. *The Leading Edge*, *28*, 24–27.

Masson, Y. J., & Pride, S. R. (2011). Seismic attenuation due to patchy saturation. *Journal of Geophysical Research*, *116*, B03206. https://doi.org/10.1029/2010JB007983

Mavko, G., Chan, C., & Mukerji, T. (1995). Fluid substitution: Estimating changes in Vp without knowing Vs. *Geophysics*, *60*, 1750–1755.

Mavko, G., & Mukerji, T. (1998). Bounds on low-frequency seismic velocities in partially saturated rocks. *Geophysics*, *63*, 918–924.

Mavko, G., Mukerji, T., & Dvorkin, J. (2009). *The rock physics handbook: Tools for seismic analysis in porous media* (2nd ed.). Cambridge: Cambridge University Press, 2nd edition.

Milani, M., Monachesi, L. B., Sabbione, J. I., Rubino, J. G., & Holliger, K. (2016). A generalized effective anisotropic poroelastic model for periodically layered media accounting for both Biot's global and interlayer flows. *Geophysical Prospecting*, *64*, 1135–1148.

Monachesi, L. B., Rubino, J. G., Rosas-Carbajal, M., Jougnot, D., Quintal, B., & Holliger, K. (2015). An analytical study of seismoelectric signals produced by 1-D mesoscopic heterogeneities. *Geophysical Journal International*, *201*, 329–342.

Müller, T. M., & Gurevich, B. (2004). One-dimensional random patchy saturation model for velocity and attenuation in porous rocks. *Geophysics*, *69*, 1166–1172.

Müller, T. M., Gurevich, B., & Lebedev, M. (2010). Seismic wave attenuation and dispersion resulting from wave-induced flow in porous rocks—A review. *Geophysics*, *75*, 75A147–75A164.

Murphy, W. F. III (1984). Acoustic measures of partial gas saturation in tight sandstones. *Journal of Geophysical Research*, *89*, 11,549–11,559.

Norris, A. N. (1993). Low-frequency dispersion and attenuation in partially saturated rocks. *International Journal for Numerical and Analytical Methods in Geomechanics*, *94*, 359–370.

Reuss, A. (1929). Berechnung der fliessgrenze von mischkristallen auf grund der plastizita tsbedingung fur einkristalle. *Zeitschrift fur Angewandte Mathematik und Mechanik*, *9*, 49–58.

Rubino, J. G., Monachesi, L. B., Müller, T., Guarracino, L., & Holliger, K. (2013). Seismic wave attenuation and dispersion due to wave-induced fluid flow in rocks with strong permeability fluctuations. *The Journal of the Acoustical Society of America*, *134*, 4742–4751. https://doi.org/10.1121/1.4824967

Toms-Stewart, J., Müller, T. M., Gurevich, B., & Paterson, L. (2009). Statistical characterization of gas-patch distribution in partially saturated rocks. *Geophysics*, *74*, WA51–WA64.

Vogelaar, B., Smeulders, D., & Harris, J. (2010). Exact expression for the effective acoustics of patchy-saturated rocks. *Geophysics*, *75*, N87–N96.

White, J. E. (1975). Computed seismic speeds and attenuation in rocks with partial gas saturation. *Geophysics*, *40*, 224–232. https://doi.org/10.1190/1.1440520

Wollner, U., & Dvorkin, J. (2016). Effective fluid and grain bulk moduli for heterogeneous thinly layered poroelastic media. *Geophysics*, *81*, D573–D584.

Wollner, U., & Dvorkin, J. (2018). Effective bulk modulus of the pore fluid at patchy saturation. *Geophysical Prospecting*, *66*(7), 1372–1383.

Wollner, U., & Mavko, G. (2017). Brown and Korringa constants for heterogeneous thinly layered poroelastic media. *Journal of Geophysical Research*, *122*, 895–905. https://doi.org/10.1002/2016JB013672